High Bandwidth Short Stroke Rotary Fast Tool Servo

R.C. Montesanti, D.L. Trumper

August 27, 2003

LAWRENCE
LIVERMORE
NATIONAL
LABORATORY

High Bandwidth Short Stroke Rotary Fast Tool Servo

Richard C. Montesanti [a, b], Professor David L. Trumper [a]
[a] Massachusetts Institute of Technology, Cambridge, MA
[b] Lawrence Livermore National Laboratory, Livermore, CA

This paper presents the design and performance of a new rotary fast tool servo (FTS) capable of developing the 40 g's tool tip acceleration required to follow a 5 micron PV sinusoidal surface at 2 kHz with a planned accuracy of 50 nm, and having a full stroke of 50 micron PV at lower frequencies. Tests with de-rated power supplies have demonstrated a closed-loop unity-gain bandwidth of 2 kHz with 20 g's tool acceleration, and we expect to achieve 40 g's with supplies providing +/- 16 Amp to the Lorentz force actuator. The use of a fast tool servo with a diamond turning machine for producing non-axisymmetric or textured surfaces on a workpiece is well known. Our new rotary FTS was designed to specifically accommodate fabricating prescription textured surfaces on 5 mm diameter spherical target components for High Energy Density Physics experiments on the National Ignition Facility Laser (NIF).

The basic topologies for a rotary fast tool servo and a linear fast tool servo are shown in **Figure 1**. A rotary fast tool servo is preferred in certain diamond-turning applications that are intolerant to the reaction force developed by a linear fast tool servo. For instance, in the present case where it is desired to produce a textured surface on a spherical workpiece a fast tool servo is mounted on a relatively slow rotary axis (B-axis) that allows the tool to engage the workpiece at all points from its "pole" to its "equator", as depicted in **Figure 2**. A rotary-type mechanism oriented with its rotation axis parallel to the B-axis generates a reaction torque on the B-axis, which can be allowed to float as a reaction mass or be locked and allowed to transmit the torque to the machine structure. In the latter case, the machine structure experiences a disturbance torque whose value does not depend on the angle of the B-axis. In contrast, a linear fast tool servo will generate a reaction force on the B-axis. This is generally not a problem when the B-axis is positioned so that the reaction force is parallel to the direction of travel of the slide carrying the B-axis. In that case the relatively heavier slide carrying the B-axis acts as a reaction mass to the linear fast tool servo. However, when the B-axis is positioned so that a component of the reaction force is perpendicular to the direction of travel of that slide, that force component is transmitted by the slide to the machine structure as a disturbance. To the extent that the tool/workpiece interaction is affected by disturbances to the machine structure, unless the reaction force is dealt with, a linear fast tool servo will thus produce variations in the desired surface texture as a function of "latitude" on a spherical workpiece.

The above discussion is quantified by comparing a conservative total moving mass rotary inertia of 100 gm-cm^2 for a rotary FTS with a 5 mm swing radius (twice the inertia of our present system) and an optimistic total moving mass of 10 gm for a linear FTS. A future design goal is to produce a fast tool servo with the 1000 g's tool acceleration needed to follow a 5 micron PV sinusoidal surface at 10 kHz. In this case the reaction torque from the rotary FTS and reaction force from the linear FTS are 20 N-m and 100 N, respectively. If the FTS is mounted on a B-axis that is allowed to float, a reaction torque causes an angular acceleration of the rotating element of the B-axis creating a tangential displacement between the surface of a spherical workpiece and the tool. Using a conservatively low rotary inertia of 0.0052 kg-m^2 for the moving element of the B-axis (e.g. a non-motorized 4 inch air bearing spindle), a 20 N-m rotary FTS reaction torque produces a negligible +/- 5 nm tangential motion between the tool and a 5 mm diameter spherical workpiece. In comparison, without an effective reaction mass between the linear FTS and the B-axis, the 100 N reaction force is transmitted directly through the B-axis as a disturbance to the machine structure, which is surely a large disturbance.

Our new high bandwidth rotary fast tool servo is shown in **Figure 3**. The swingarm carries a diamond tool at a swing radius of 5 mm and has a full-travel angle of +/- 5 mrad. The small rotation angle allows using over-constrained crossed-flexures to guide the rotary motion. A total of eight flexures are used, four above the tool and four below it. The inner ends of the flexures are fixed to the swingarm, and the outer ends are fixed to the base. To ease manufacturing and assembly, pairs of collinear flexures are formed from a single piece, as best seen in **Figure 4**. Each flexure is a 0.15 mm thick piece of 1095 blue tempered spring steel that has been polished along its long axis to minimize initiation of fatigue cracks. Each flexure is pre-tensioned with a 50 N load before clamping the ends. This pre-tension, along with the over-constrained arrangement, is intended to provide a well-defined axis of rotation that does not wander when the swingarm is rotated. The measured stiffness at the plane of the tool along the

centerline is 22 and 15 N/micron in the axial and radial directions, respectively. The 5 mm swing radius combined with a moving mass rotational inertia of 51 gm-cm^2 results in an effective linear mass of 0.2 kg as seen at the tool tip. The expected dynamic stiffness of the tool at 2 kHz is on the order of 20 N/micron. The parasitic transverse motion of the tool tip is only +/- 62 nm for the full travel of +/- 25 micron, making it negligible and thus simplifying CNC programming for machining a workpiece. A drawback of using a small swing radius is that the actuator acceleration is de-magnified as reflected into tool tip acceleration.

Our new rotary fast tool servo uses a commercially available small diamond tool weighing 0.4 gm (diamond plus steel shank), shown in Figure 4. The sides of the tool shank form a 30 degree taper angle that is received by a tapered slot in the swingarm. To insure a high stiffness connection between the tool and swingarm, the sides of the tool shank are relieved to provide four distinct areas of contact with the swingarm, two in the front and two in the rear. A leaf spring is used to transmit the hold-down force from a setscrew to the center of the tool shank.

We used a commercially available moving-magnet galvanometer for the actuator, and built our own power amplifier and current-loop compensation circuit. **Figure 5** shows a block diagram of the control system and the measured small signal closed-loop response of the tool position. The inner current loop has a crossover frequency of 30 kHz, essentially removing the electrical dynamics of the power amplifier and actuator at frequencies up to the desired 2 kHz. We designed and used an integral rotary viscous damper consisting of a thin circular plate attached to the bottom of the swingarm. A 0.1 mm gap between each face of the circular plate and the adjacent stationary surface is filled with heavy grease. This damper significantly reduced the effect of a 5 kHz resonance between the swingarm and the moving element of the actuator, making it possible to use a simple PI controller for stabilizing the outer tool position loop with a crossover frequency of 1 kHz. The inner loop was implemented with analog components, while the outer loop compensation is implemented with a PC-based digital controller using an 80 kHz sampling rate. The position of the tool is measured by a pair of eddy current sensors operating differentially and looking at the back of the swingarm on either side of the axis of rotation and near the elevation of the tool. This is best seen in **Figure 6**, which shows the swingarm and diamond tool engaging a workpiece during the first cutting test. The eddy current sensor amplifier produces a +/- 10 V signal for the +/- 25 micron tool swing, and has a noise level of 4 mV PV which corresponds to +/- 10 nm PV.

During the first cutting test shown in Figure 6 the tool was commanded to hold a constant position while facing the workpiece, so that the robustness of the FTS mechanism and the control system could be benchmarked. We used a diamond tool with a 25 micron nose radius and a federate of 2.5 micron/rev. This leads to a rather coarse theoretical finish of 30 nm PV, but since we were exercising fairly loose control over the thermal environment at the work zone we chose to use a relatively fast feed rate to better assure a constant depth of cut across the 9 mm diameter part. The resulting surface on the 6061-T6 aluminum workpiece (not the most ideal material to diamond turn, but readily available) is also shown in Figure 6. Preliminary measurements indicate that the diamond turning groove depths match the theoretical 30 nm PV, but are superimposed on a 60 nm PV waviness with a 30 micron spatial wavelength, resulting in a 13 nm rms roughness for a 0.18 mm scan length. The 30 micron waviness corresponds to a 0.7 Hz disturbance. Likely culprits are least-bit dithering of the non-locked in-feed slide, mechanical ground noise through the passive air isolators, and spindle air pressure fluctuations.

Additional cutting tests will be performed to determine the ability of our new rotary FTS to produce sinusoidal surfaces on the face and diameter of a workpiece at 2 kHz. Follow-on work includes implementing advanced controller algorithms such as Feedfoward cancellation to account for phase delay at higher frequencies and Adaptive Feedfoward Cancellation to reduce following error and reject disturbances at select frequencies. We also plan to design, build, and test a new prototype intended to provide the same stroke at 10 kHz.
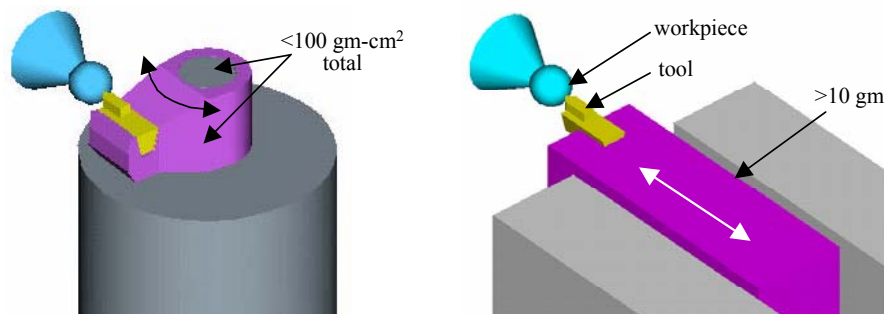

Figure 1: Basic topologies for Rotary (left) and Linear (right) fast tool servos.
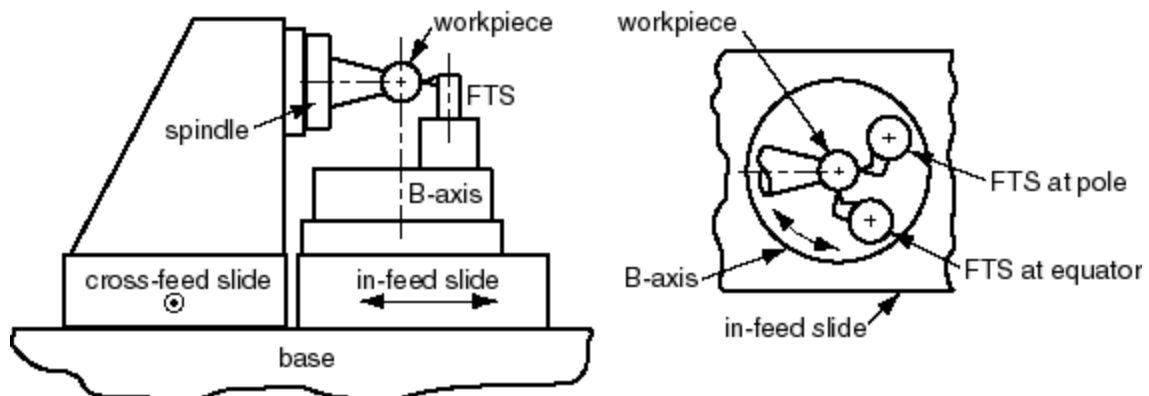
Figure 2: Sketch of a fast tool servo set up on a two-axis lathe with a B-axis for machining a spherical workpiece. Side view (left). Top view (right) showing tool at equator and at pole of workpiece.
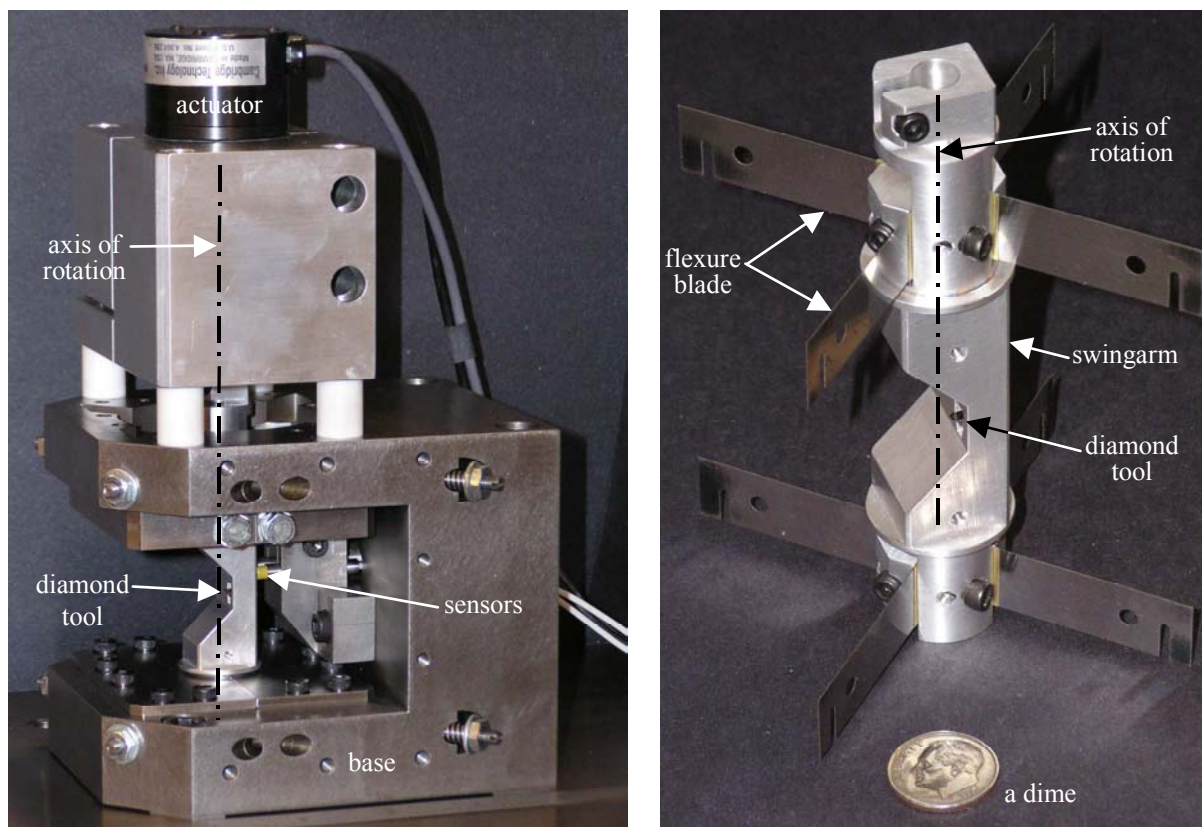

Figure 3: Our 2 kHz rotary fast tool servo (left), and its rotating element not including the actuator (right).
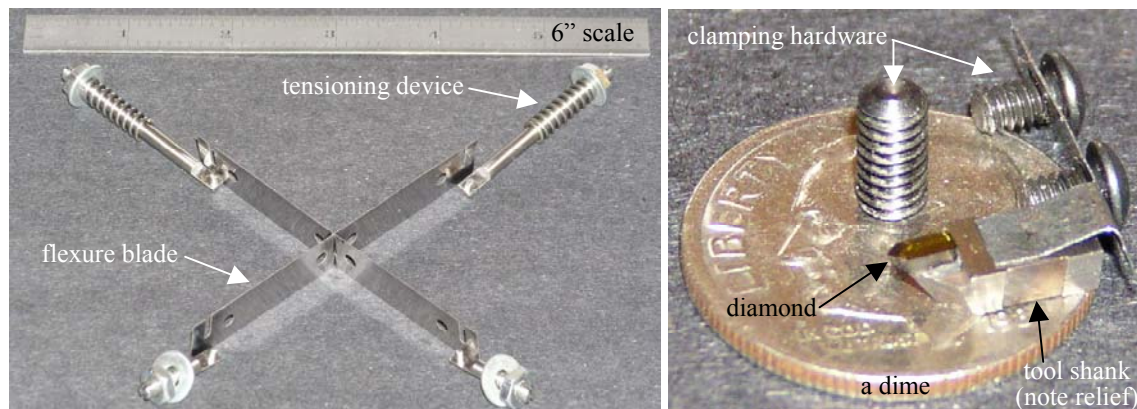
Figure 4: Four flexure blades and tensioning devices (left), and diamond tool with clamping hardware (right).
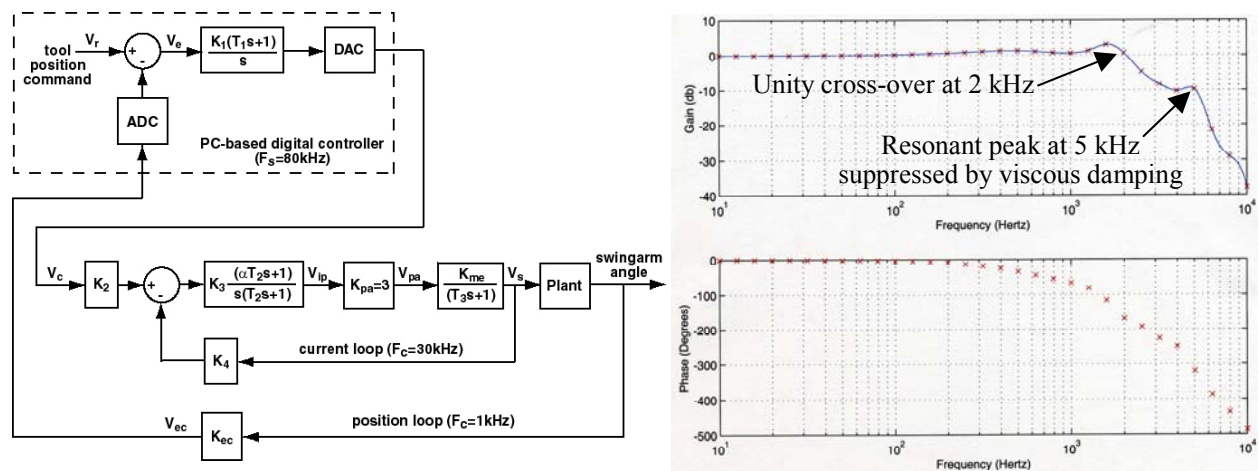

Figure 5: Control system block diagram (left), and measured small-signal closed-loop response (right).
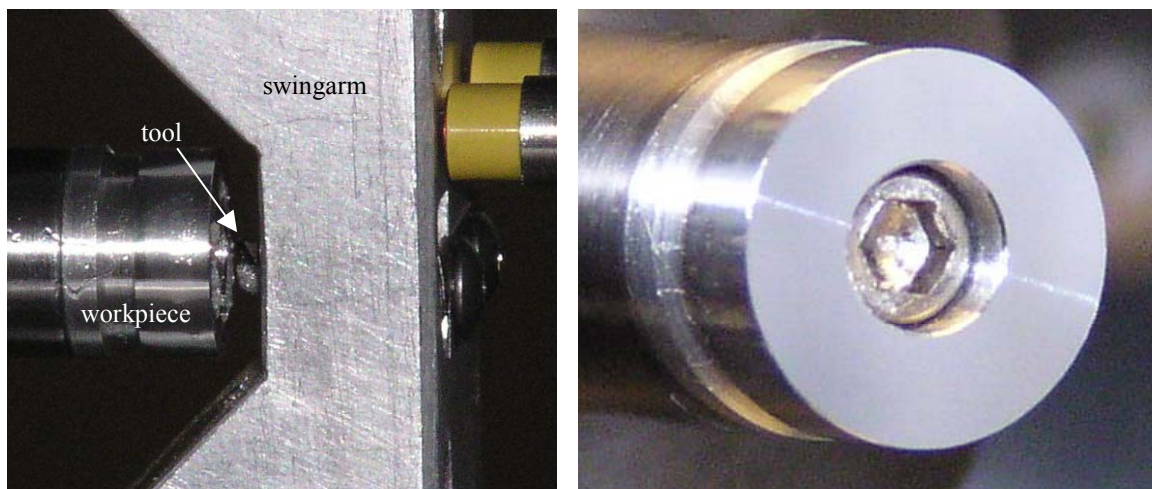

Figure 6: First cutting test with our 2 kHz rotary FTS. Side view (left) and face view of part (right).